# On vaporization in laser material interaction

Hyungson Ki

Citation: J. Appl. Phys. **107**, 104908 (2010); doi: 10.1063/1.3428966
View online: http://dx.doi.org/10.1063/1.3428966
View Table of Contents: http://jap.aip.org/resource/1/JAPIAU/v107/i10
Published by the AIP Publishing LLC.

# On vaporization in laser material interaction

Hyungson Ki[a)]
*School of Mechanical and Advanced Materials Engineering, Ulsan National Institute of Science and Technology, Ulsan, South Korea*

(Received 7 October 2009; accepted 15 April 2010; published online 26 May 2010)

In this article, vaporization processes in the laser interaction with materials are studied theoretically and computationally, focusing on evaporation and homogeneous bubble nucleation. Simulations are carried out using the Redlich–Kwong equation of state and temperature-dependent material property models that can be used up to the critical point. From theoretical considerations, four important temperatures are identified in the understanding of laser material interaction. This study also shows that there are upper limits to the amount of energy that can be consumed by vaporization, which takes place at a temperature that is lower than the material's critical point. This study also discusses the transition from the thermal mode of ablation to the nonthermal mode in terms of the energy capacity of homogeneous boiling. © *2010 American Institute of Physics*. [doi:10.1063/1.3428966]

## I. INTRODUCTION

In the laser interaction with materials, vaporization plays a critical role. Although mass removal due to melt flow is important for a wide range of laser intensity values, vaporization is a more dominant ablation mode at higher intensity values.[1] Two types of vaporization are believed to take place in most high-energy ablation processes: evaporation and homogeneous boiling.[2] Evaporation starts to occur at the surface when the surface temperature reaches the boiling temperature. Homogeneous boiling (or homogeneous bubble nucleation), on the other hand, takes place inside the melt when the liquid melt is highly superheated and the surface tension becomes very small near the critical point temperature.[1] In certain cases, homogeneous boiling occurs so rapidly and uncontrollably that it is called explosive boiling. Because the evaporation is very rapid, the liquid is highly superheated and the vaporization processes take place in the metastable region.

It is no exaggeration to say that vaporization processes are at the heart of laser material interaction and many laser material processing applications, but due to the complexity of the problem, the understanding of those processes is relatively limited. In particular, homogenous boiling is largely unexplored compared to evaporation and has been neglected in many previous studies.

In order to study vaporization in laser ablation, temperature-dependent material properties over a wide temperature range must be employed because the vaporization in laser ablation typically occurs at very high temperatures and material properties change drastically near the critical point. For example, surface tension and the latent heat of vaporization both vanish at the critical point since the distinction between liquid and vapor no longer exists; the recoil pressure induced by vaporization is far from saturation pressure because vaporization takes place very rapidly. Therefore, without using accurate material properties near the critical point we cannot expect to obtain reliable results. As far as the author knows, however, the importance of using accurate material properties near the critical point has not been adequately addressed in most previous studies.

In this article, the author studies the vaporization processes theoretically and computationally, and presents some insights into the roles and characteristics of vaporization processes in the laser interaction with materials. Especially, an emphasis is placed on accurate modeling of material properties over a wide range of temperatures up to the critical point using reduced variables (e.g., pressure and temperature normalized by their respective critical point values). This study identifies four important temperatures near the critical point, and also discusses the transition from the thermal ablation mode to the nonthermal mode. This study is conducted for iron. However, because reduced variables are employed, the results could be at least qualitatively applied to other materials according to the principle of corresponding states.

## II. MATHEMATICAL MODEL

One of the most important tasks in the study of laser material interaction is the evaluation of material properties at high temperatures because the actual ablation process takes place near the critical point and material properties change drastically there. As well known, when a high-density laser beam irradiates on a target material, generally four phases of the material (solid, liquid, vapor, and plasma) appear simultaneously because the intense electromagnetic field of the laser beam drives the temperature up past the material's critical point. Therefore, in order to capture important physics, it is essential to use reasonably good material property models that are valid at those high temperatures. In this study, material properties, such as density, latent heat of vaporization, and surface tension are theoretically extended to the critical point using material property models, so that accurate and reliable results can be obtained. The temperature-dependent density is obtained by simultaneously solving the Redlich–Kwong equation of state[3] and the saturation curve by Riedel.[4] For the latent heat of vaporization, Watson's model[5] is employed. Surface tension is known to be one of the most

[a)]Electronic mail: hski@unist.ac.kr.

 

important material properties in laser material interaction, and in this study, the two-parameter model by Somayajulu[6] is employed with the surface tension data in Ref. 7 is used to determine the parameters. The critical point temperature and pressure of iron used are 9250 K and 8750 bar,[8] respectively. In this way, the vaporization processes up to the critical point can be simulated using realistic material properties.

With the aforementioned temperature-dependent material property models, vaporization models can be used from the room temperature to the critical point. In this study, Knight's evaporation model with the backscattering flux[9] is employed for evaporation, and classical nucleation theory[10] is used to model homogeneous nucleation.

At the evaporating surface, there exists a thin layer of several mean free paths, called the Knudsen layer, across which the temperature, density, and pressure of the evaporating particles are discontinuous. According to Knight,[9] these discontinuities can be modeled as follows:

$$\frac{T_v}{T_s} = \left[ \sqrt{1 + \pi\left(\frac{\gamma_v - 1}{\gamma_v + 1}\frac{m}{2}\right)^2} - \sqrt{\pi}\left(\frac{\gamma_v - 1}{\gamma_v + 1}\frac{m}{2}\right) \right]^2, \tag{1}$$

$$\frac{\rho_v}{\rho_s} = \sqrt{\frac{T_s}{T_v}}\left[\left(m^2 + \frac{1}{2}\right)\exp(m^2)\mathrm{erfc}(m) - \frac{m}{\sqrt{\pi}}\right] + \frac{1}{2}\frac{T_s}{T_v}[1 - \sqrt{\pi}m\,\exp(m^2)\mathrm{erfc}(m)], \tag{2}$$

$$\frac{p_v}{p_{\mathrm{air}}} = 1 + \gamma_{\mathrm{air}} M_v \frac{a_v}{a_{\mathrm{air}}}\left\{\frac{\gamma_{\mathrm{air}} + 1}{4} M_v \frac{a_v}{a_{\mathrm{air}}} + \left[1 + \left(\frac{\gamma_{\mathrm{air}} + 1}{4} M_v \frac{a_v}{a_{\mathrm{air}}}\right)^2\right]^{1/2}\right\}. \tag{3}$$

In Eqs. (1)–(3), $\gamma$ is the ratio of specific heats, $a$ is the sound speed, and subscripts $s$, $v$, and air denote the start point of the Knudsen layer at the evaporating surface, the end point of the Knudsen layer (including the rarefaction fan if the flow is supersonic), and outside air, respectively. Also, $m = \sqrt{\gamma_v/2}M_v$, where $M$ is the Mach number. Then, the evaporation mass flux per unit surface area is computed as

$$\dot{m}''_{\mathrm{evap}} = \rho_s\sqrt{\frac{RT_s}{2\pi}} - \rho_v\sqrt{\frac{RT_v}{2\pi}}\beta A, \tag{4}$$

where $R$ is the gas constant, and

$$A = \sqrt{\pi}m[\mathrm{erf}(m) - 1] + \exp(-m^2),$$

$$B = (2m^2 + 1)[1 - \mathrm{erf}(m)] - \frac{2}{\sqrt{\pi}}m\,\exp(-m^2),$$

$$\beta = \frac{2(2m^2 + 1)\sqrt{T_v/T_s} - 2\sqrt{\pi}m}{A + \sqrt{T_v/T_s}B}. \tag{5}$$

Implementation details can be found in Refs. 9 and 11.

In classical nucleation theory,[10] the critical radius of a bubble is calculated as

$$R_{\mathrm{crit}} = \frac{2\sigma}{p_{\mathrm{sat}}(T_l)\exp\{[p_l - p_{\mathrm{sat}}(T_l)]/(\rho_l R T_l)\} - p_l}. \tag{6}$$

Here, $T_l$, $p_l$, $p_{\mathrm{sat}}(T_l)$, $\rho_l$, $\sigma$, and $R$ are liquid temperature, liquid pressure, saturation pressure at $T_l$, density of liquid, surface tension, and the gas constant, respectively. Then, the homogeneous nucleation rate ($\dot{H}'''$) and the mass flux per unit volume ($\dot{m}'''_{\mathrm{boiling}}$) can be computed by

$$\dot{H}''' = N_l\left[\frac{6\sigma}{\pi m_m(2 - p_l/p_{\mathrm{bubble}})}\right]^{1/2}\exp\left[\frac{-4\pi R_{\mathrm{crit}}^2\sigma}{3k_B T_l}\right], \tag{7}$$

$$\dot{m}'''_{\mathrm{boiling}} = m_{\mathrm{bubble}}\dot{H}''', \tag{8}$$

where $N_l$, $m_m$, $p_{\mathrm{bubble}}$, $k_B$, and $m_{\mathrm{bubble}}$ are the number of liquid molecules per unit volume, mass of one molecule, pressure in the vapor bubble, Boltzmann constant, and the mass of the bubble.

In laser material interaction, predicting the surface pressure generated by evaporation is a very important task because the entire process is far from equilibrium. This pressure is known as recoil pressure, and from this pressure and the surface temperature the thermodynamic state can be fixed and the degree of superheat can be calculated. In this study, the recoil pressure is calculated in the following way.

At the evaporating surface, as stated earlier, macroscopic properties are discontinuous across the Knudsen layer. The evaporating (forward) mass flux and backscattering (backward) mass flux across the layer both contribute to the surface pressure, i.e., the recoil pressure. At equilibrium, the forward and backward mass fluxes will equally contribute to the recoil pressure, and the recoil pressure will be same as the saturation pressure at the given surface temperature, i.e., $p_{\mathrm{sat}}(T_s)$. If there is only the forward mass flux (e.g., evaporation in vacuum), the recoil pressure will be roughly equal to $(1/2)\rho_f u_f^2$ from Newton's third law of motion, which is much smaller than the saturation pressure. Here, $\rho_f$ and $u_f$ are the density and velocity of the forward mass flux. In an actual heating process, the recoil pressure will be between these two extremes. In this study, with the modification of the author's previous model,[1] the recoil pressure is approximated from the kinetic energy exchange between the evaporating and condensing backscattering fluxes across the Knudsen layer as follows:

$$p_{\mathrm{rec}} \cong \frac{\rho_f u_f^2 + \rho_b u_b^2}{2\rho_f u_f^2} p_{\mathrm{sat}}(T_s). \tag{9}$$

Here, $\rho_b$ and $u_b$ are the density and velocity of the backward (backscattering) mass flux. Note that $\rho_f$, $\rho_b$, $u_f$, and $u_b$ are obtained from Knight's evaporation model.[9] From Eq. (9), we can learn that the surface gets superheated when the backward flux is smaller than the forward flux.

In this study, because this study only focuses on two vaporization processes, the absorption characteristic of a ma-

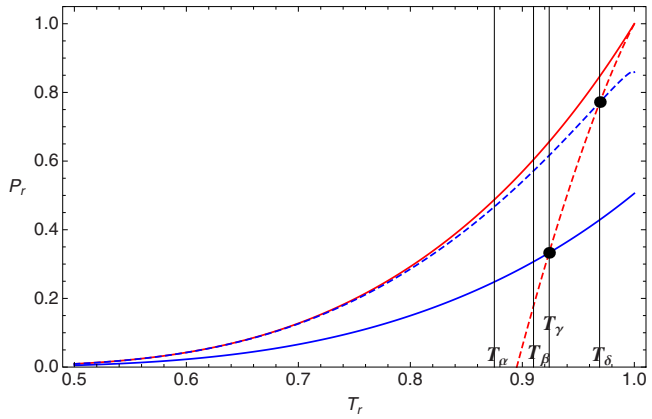


FIG. 1. (Color online) Phase diagram for the laser interaction with materials.

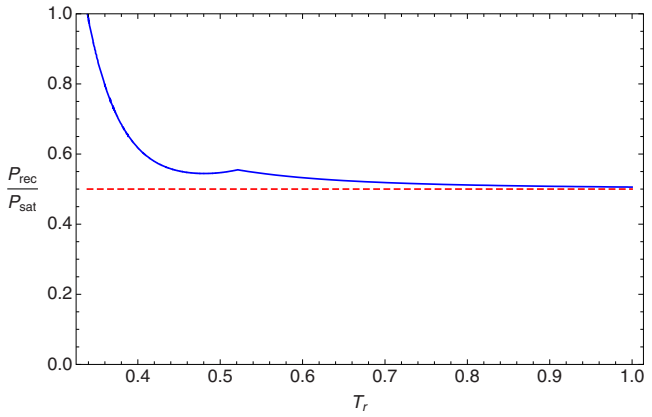


FIG. 2. (Color online) Ratio of the recoil pressure to the corresponding saturation pressure.

terial is not considered and the laser intensity values stated in this article are the actual intensity values absorbed at the material surface.

## III. RESULTS AND DISCUSSION

In this study, laser material interaction is simulated with an iron target. However, to generalize the results as much as possible, reduced variables are used. In other words, thermodynamics properties, such as temperature, pressure, and density, are normalized with respect to their critical point values. As well known, when reduced variables are used in thermodynamics, the obtained results can be qualitatively applied to other materials from the principle of corresponding states.

Figure 1 shows the saturation pressure (solid red) and the recoil pressure (solid blue) plotted together as functions of the surface temperature. In Fig. 1, the saturation curve is calculated by Riedel's model[4] and the recoil pressure is predicted by Eq. (9). In Fig. 1, $T_r$ and $p_r$ are reduced temperature and reduced pressure respectively, which are defined as

$$T_r = \frac{T}{T_{CP}} \quad \text{and} \quad p_r = \frac{p}{p_{CP}}, \tag{10}$$

where $T_{CP}$ and $p_{CP}$ are the critical point temperature and pressure. As expected, the surface pressure is much lower than the corresponding saturation pressure, so the surface is highly superheated. Note that, as pointed out in Ref. 1, the liquid layer is very thin in most laser ablation processes, and the pressure across the liquid layer is almost constant and equal to the recoil pressure. In Fig. 1, the red dashed line is the spinodal calculated from the Redlich–Kwong equation of state. Because the liquid layer is highly superheated, the actual heating curve (solid blue) meets the spinodal at a place other than the critical point. In this case it takes place at $T_r = 0.924$, which is marked by one of the two black solid circles. This means that beyond this temperature along the heating curve the liquid enters the spinodal region. As well known,[10] the spinodal region is an unstable region and the material in this region is not sustainable. Therefore, due to the rapid heating and low surface pressure, it is as if the effective critical point has moved to this point. Let us define this temperature as $T_\gamma$. Also, note that at this point pressure is only 0.333 $p_{CP}$, which is probably the maximum achievable liquid pressure during the rapid laser heating.

Figure 2 is the calculated ratio of the recoil pressure (solid blue line in Fig. 1) to the saturation pressure (solid red line in Fig. 1), from which we can measure the degree of superheat: the smaller it is, the more superheated the liquid is. Apparently, at the normal boiling temperature (for iron 3133 K or $T_r = 0.339$), the surface is saturated but as the temperature increases it becomes more and more superheated. At the critical point, the recoil pressure is only about 50.6% of the corresponding saturation pressure, which agrees well with literature.[12] This is ascribed to the fact that across the Knudsen layer the backward flux is very small compared to the forward flux (like the evaporation in vacuum). Also, there is a little spike at around $T_r = 0.521$. This spike is caused by a change in flow structure outside the Knudsen layer: at this temperature the flow Mach number becomes one, and the flow becomes supersonic from subsonic.

In Fig. 3, the critical bubble radius for homogeneous nucleation[10] is calculated and plotted versus liquid temperature. In classical nucleation theory,[10] only bubbles greater than this radius can grow further and smaller bubbles collapse. As well known, the critical radius decreases as the

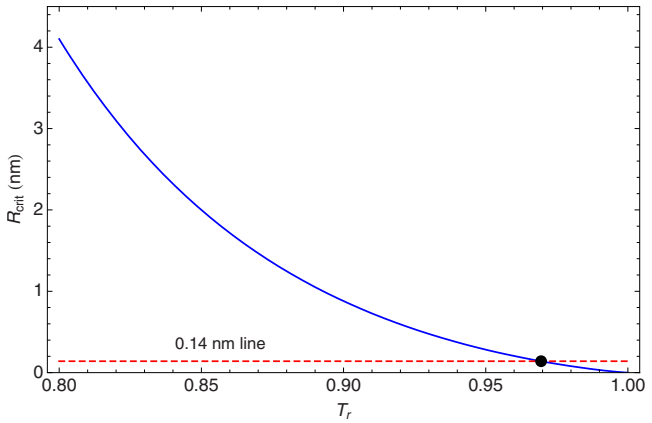


FIG. 3. (Color online) The critical bubble radius for homogeneous nucleation.

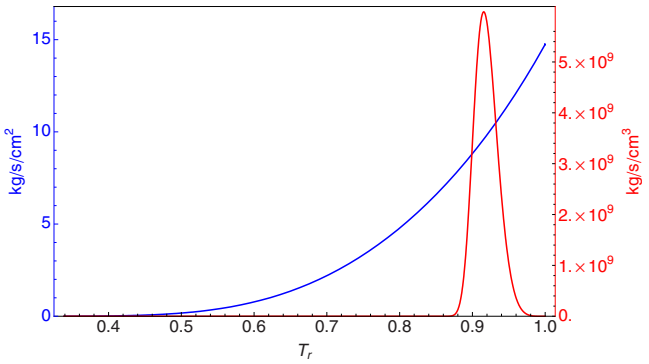


FIG. 4. (Color online) Mass fluxes due to evaporation (blue) and homogeneous bubble nucleation (right red curve).

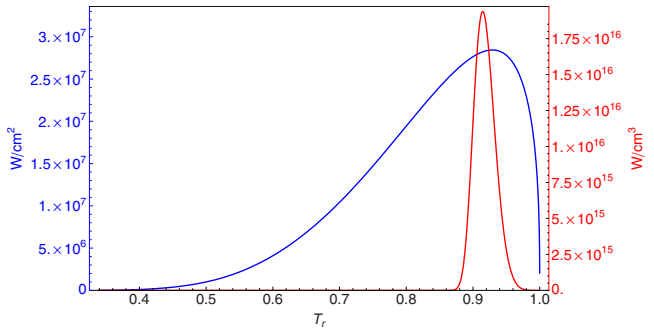


FIG. 5. (Color online) Phase-change energy fluxes due to evaporation (blue) and homogeneous bubble nucleation (right red curve).

temperature increases. For comparison, the curve is plotted together with a 0.14 nm indicator line, which is the radius of an iron atom.[13] The two curves meet at $T_r$=0.969 (black solid circle), which means that the critical radius equals the radius of an iron atom at that temperature. This point has a special meaning because from this temperature on a bubble does not need to grow at all to reach the critical radius. It is a one-atom bubble, and it is already at the critical radius. The bubble growth is automatic. In other words, theoretically, the liquid atom is vapor already as soon as it reaches this point. Let us call this temperature as $T_\delta$. ($T_\delta$ is shown in Fig. 1.) However, this temperature is greater than $T_\gamma$, so it may not be achievable in rapid laser heating. Note that in Fig. 3 the critical radius smaller than the atom radius is meaningless, so it should be let equal to the atom radius beyond $T_\delta$. In addition, beyond $T_\delta$ it is not possible to define the surface tension of the critically sized bubble.

Using the critical radius given in Fig. 3, the pressure inside the bubbles of critical radius is calculated using the Young–Laplace equation as

$$p_{\text{bubble}} = p_l + \frac{2\sigma}{R_{\text{crit}}}, \tag{11}$$

and plotted versus liquid temperature in Fig. 1 (dashed blue line). It is interesting to see that this pressure is close to but is always smaller than the saturation pressure. The bubble pressure curve deviates more and more from the saturation curve as temperature goes up. Therefore, even when the vapor bubbles are exposed to outside, the surface pressure will be always less than the saturation pressure. Also, this bubble pressure curve meets with the spinodal curve at around $T_r$ =0.969, which is interestingly the same as $T_\delta$ that was defined as the temperature where the critical bubble radius is the radius of an iron atom. Note that this may be by coincidence but makes some sense intuitively. So, we can say that loosely when the critical bubble radius equals the iron atom radius, the vapor bubble enters the spinodal region.

Figures 4 and 5 show the mass fluxes and energy fluxes due to evaporation and homogeneous bubble nucleation. Because evaporation is a surface phenomenon and homogeneous boiling is a volumetric phenomenon, graphs are plotted with different scales and units. In this study, it is assumed that in homogeneous boiling bubbles leave the liquid region at the critical radius. This is a reasonable assumption because in such a rapid heating there is not much time for bubbles to grow after they reach the critical radius, especially when intensities are very high.

As seen in Fig. 4, the mass flux characteristics of two vaporization modes are completely different. In this study, the evaporation mass flux is the net evaporating mass flux across the Knudsen layer calculated by Eq. (4), and the mass flux due to homogenous boiling is calculated using Eq. (8). The evaporation mass flux, starting from the normal boiling point, increases in an exponential manner up to the critical point while the mass flux due to homogeneous boiling is suddenly initiated at around $T_r$=0.85, peaks at $T_r$=0.916, and then goes to zero at the critical point. It is interesting to see that the homogeneous boiling mass flux vanishes at the critical point. Mathematically, this is because the critical bubble radius decreases faster than the increase in the number of nuclei generation. Beyond $T_\delta$, however, the homogeneous boiling flux might be mathematically meaningless.

Figure 5 shows the energy flux due to the two modes of vaporization. In this study, energy fluxes only include the energies due to liquid-vapor phase change, such as the latent heat of vaporization. As seen in Fig. 5, the evaporation energy flux also increases in an exponential manner with time, but unlike the mass flux, it peaks at around $T_r$=0.929 and goes to zero at the critical point. This is obvious because the latent heat of vaporization vanishes at the critical point and the evaporation energy flux per unit surface area is calculated as follows:

$$\dot{e}''_{\text{evap}} = \dot{m}''_{\text{evap}} L_v. \tag{12}$$

Here, $L_v$ is the latent heat of vaporization. Note that at the critical point the distinction between liquid and vapor vanishes, therefore, there is no latent heat of vaporization. The energy flux due to homogeneous nucleation has a similar pattern to its mass flux. To form a bubble, now two types of energy are required: free energy to construct a surface[10] and the latent heat of vaporization, so the homogeneous boiling energy flux per unit volume is written as follows:

$$\dot{e}'''_{\text{boiling}} = \dot{m}'''_{\text{boiling}} L_v + \frac{4}{3}\pi\sigma R_{\text{crit}}^2 \dot{H}'''. \tag{13}$$

Here, both $\dot{m}'''_{\text{boiling}}$ and $\dot{H}'''$ are calculated from classical nucleation theory. Since both latent heat and surface tension go to zero at the critical point, there is no energy flux associated with phase change there. This is clearly shown in Fig.

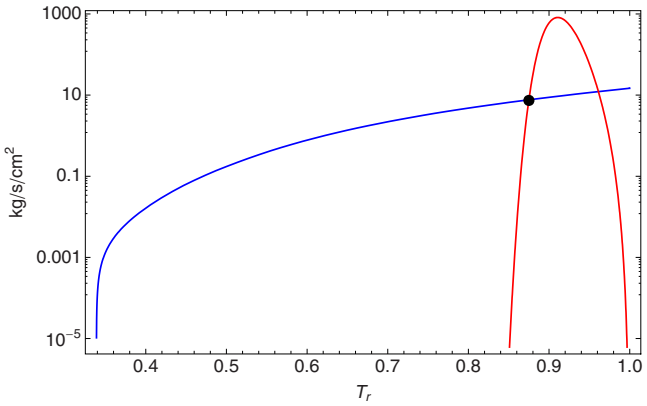


FIG. 6. (Color online) Mass fluxes per unit surface area due to evaporation (blue) and homogeneous bubble nucleation (right red curve).

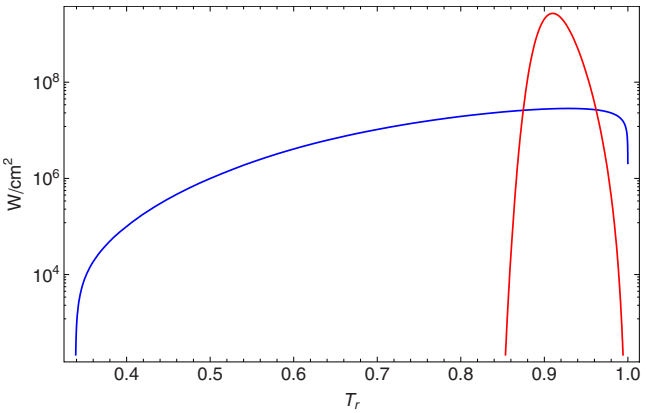


FIG. 7. (Color online) Energy fluxes per unit surface area due to evaporation (blue) and homogeneous bubble nucleation (right red curve).

5, where the curve has the maximum volumetric energy flux at $T_r$=0.915, and after that, goes to zero at the critical point. Here, one thing about vaporization processes in laser heating should be noted: both modes of vaporization are finite in terms of mass and energy removal capacity and have maximum fluxes at the temperatures that are lower than the critical point temperature. In other words, vaporization processes have a certain energy capacity, beyond which other mechanisms are required to absorb energy further.

To compare homogeneous boiling fluxes directly with evaporation fluxes, the former need to be converted to area fluxes (per cm$^2$) by multiplying the "effective boiling thickness," which is defined as an equivalent liquid layer thickness, which, when multiplied by the homogeneous boiling fluxes at the surface temperature and pressure, yields the total fluxes per unit surface area. Since it is difficult to calculate this thickness precisely, it is assumed that the effective boiling thickness is equal to the critical bubble diameter at the surface temperature and pressure. In other words, it is assumed that only one layer of bubbles at the surface is removed due to homogeneous nucleation. This assumption is reasonable because of two reasons. First, since the pressure across the liquid layer is constant at the recoil pressure, going into the liquid layer, the degree of liquid superheat decreases (which will negatively effect the homogeneous bubble nucleation at places away from the liquid-vapor interface) so the homogeneous nucleation rate will decrease sharply. Second, the liquid layer thickness decreases quickly with increasing surface temperature (i.e., the temperature gradient becomes much steeper at higher laser fluences).

In Figs. 6 and 7, homogeneous boiling mass and energy fluxes are calculated per unit surface area, by multiplying the effective boiling thickness, and are plotted together with corresponding evaporation fluxes. Because now the same units are used, direct comparisons are possible. Due to the huge difference in scales, logarithmic plots are used. Overall, patterns are very similar to those shown in Figs. 4 and 5, but now we can make several important comparisons about the two vaporization processes.

First of all, as mentioned earlier, vaporization processes are limited mass removal mechanisms. As seen in Fig. 6, contrary to the common sense, there exist maximum ablation speeds due to vaporization. In the case of iron, the maximum ablation speed (or maximum mass removal rate) due to evaporation is 14.75 kg/s/cm$^2$ at $T_r$=1, and the maximum ablation speed due to homogeneous boiling is 818.5 kg/s/cm$^2$ when $T_r$=0.911. In the same way, there are upper limits to mass fluxes. Also, in Fig. 6, the intersection of the two curves is where the change in the ablation speed takes place. Let us define this temperature $T_\alpha$=0.875, which is the point where two vaporization modes equally contribute to the mass removal and a change in mass removal mode is beginning to take place ($T_\alpha$ is shown in Fig. 1).

In Fig. 7, the maximum energy flux due to evaporation is $2.84\times10^7$ W/cm$^2$ at $T_r$=0.929 while the maximum energy flux due to homogeneous boiling is $2.70\times10^9$ W/cm$^2$ at $T_r$=0.910. Therefore, homogeneous boiling is about two orders of magnitude higher than evaporation in terms of energy capacity. In the case of an iron target, up to $2.84\times10^7$ W/cm$^2$ can be taken care of by evaporation, but beyond that intensity homogeneous bubble nucleation will be the primary mechanism. In the same way, homogeneous boiling can absorb energy intensities of up to $2.70\times10^9$ W/cm$^2$, but beyond that another energy absorption mechanism is required. The author believes that this is the maximum energy intensity that thermal processes can take care of, so beyond this the material breaks down and becomes ionized. The temperature where the maximum energy flux due to homogeneous boiling takes place is important, so let us define this temperature as $T_\beta$ ($T_\beta$ is shown in Fig. 1). Note that all these intensity values are the actual intensity values at the surface neglecting the absorption characteristic of the material. Therefore, the real laser intensity will be much higher (roughly one order higher in the case of a metal surface) than these values to have the same effects.

It is somewhat surprising that the energy removal capacity is highest at $T_\beta$, not at $T_{CP}$. In this case, $T_\beta$ is 0.910, and once a material reaches this point it is believed that a breakdown is beginning to take place. Hence, as the temperature rises past $T_\beta$, nonthermal ablation mechanisms must come into play. Therefore, depending on interaction parameters $T_\beta$ could be practically the maximum temperature a material can attain. Note that as reported by Lim *et al.*[14] fluid flow is the most efficient mode of mass removal and requires relatively

small amounts of energy, so it is believed that even with the fluid flow these results are not much different from what is discussed here.

## IV. CONCLUSION

In summary, four temperatures have been indentified in terms of evaporation and homogeneous boiling processes: $T_\alpha$=0.875, $T_\beta$=0.910, $T_\gamma$=0.924, and $T_\delta$=0.969. These temperatures have been obtained for iron, but they should be qualitatively applicable to other materials because reduced variables were used in this study. $T_\alpha$ is the temperature where a change in vaporization mode takes place from evaporation to homogeneous boiling. $T_\beta$ is the temperature where the maximum amount of energy can be absorbed by a thermal process. Beyond that, a nonthermal process will take over. $T_\gamma$ is the temperature where the liquid under intense laser heating enters the spinodal region. $T_\delta$ is the temperature where the vapor inside the bubble enters the spinodal region. At this temperature, the critical bubble radius is equal to the radius of an iron atom. Note that the results are not limited to laser material interaction and can be applicable to other high intensity energy interaction with materials, such as electrical discharge machining.

## ACKNOWLEDGMENTS

This work was supported by the development program of the local science park funded by the Ulsan Metropolitan City and the Ministry of Education, Science, and Technology of Korea.

[1]H. Ki, P. S. Mohanty, and J. Mazumder, J. Phys. D: Appl. Phys. **34**, 364 (2001).
[2]A. Miotello and R. Kelly, Appl. Phys. Lett. **67**, 3535 (1995).
[3]O. Redlich and J. N. S. Kwong, Chem. Rev. **44**, 234 (1949).
[4]L. Riedel, Chem.-Ing.-Tech. **26**, 83 (1954).
[5]K. M. Watson, Ind. Eng. Chem. **35**, 398 (1943).
[6]G. R. Somayajulu, Int. J. Thermophys. **9**, 559 (1988).
[7]B. J. Keene, Int. Mater. Rev. **38**, 157 (1993).
[8]M. Beutl, G. Pottlacher, and H. Jager, Int. J. Thermophys. **15**, 1323 (1994).
[9]C. J. Knight, AIAA J. **17**, 519 (1979).
[10]V. P. Carey, *Liquid-Vapor Phase Change Phenomena* (Hemisphere, Bristol, PA, 1992).
[11]H. Ki, P. S. Mohanty, and J. Mazumder, Metall. Mater. Trans. A **33**, 1817 (2002).
[12]V. A. Batanov, F. V. Bunkin, A. M. Prokhorov, and V. B. Fedorov, Sov. Phys. JETP **36**, 311 (1973).
[13]http://www.webelements.com
[14]D. J. Lim, H. Ki, and J. Mazumder, J. Phys. D: Appl. Phys. **39**, 2624 (2006).